Water Resources Research

RESEARCH ARTICLE
10.1029/2024WR037507

Special Collection:
Integrating In Situ, Remote Sensing, And Physically Based Modeling Approaches to Understand Global Freshwater Ice Dynamics

Assessing the Potential for Medium-Range Ice Forecasts in the Laurentian Great Lakes

A. J. Yeo[1], E. J. Anderson[1], C. Jablonowski[2], D. M. Wright[3], G. E. Mann[4], A. Fujisaki-Manome[5], B. Mroczka[3], and D. Titze[3]

[1]Hydrologic Science and Engineering, Colorado School of Mines, Golden, Colorado, USA, [2]Climate and Space Sciences and Engineering, University of Michigan, Ann Arbor, Michigan, USA, [3]Great Lakes Environmental Research Laboratory, National Oceanic and Atmospheric Administration, Ann Arbor, Michigan, USA, [4]National Weather Service WFO-Detroit, National Oceanic and Atmospheric Administration, White Lake, Michigan, USA, [5]Cooperative Institute for Great Lakes Research, University of Michigan, Ann Arbor, Michigan, USA

Abstract Real-time forecasted ice information for large lakes, such as the Great Lakes, is critical for essential operations, such as ice breaking, commercial navigation, search and rescue, and oil spill response. Existing forecast products for large lake ice conditions are not available for medium-range time horizons (5–16 days out), yet they could provide important information for decision making, particularly for ice breaking and spill responses. In addition, ice forecasts for Earth's largest lakes at these timescales could be important for Medium-Range Weather (MRW) forecasting. However, the skill of existing operational products in predicting ice conditions at MRW timescales has not been studied. This work aims to determine how well ice forecasts from a coupled large lake hydrodynamic-ice model perform for MRW forecast horizons. Simulations were carried out for the 2022 Great Lakes ice season, using 8 different 16-day forecast periods. Forecast results were compared to observations of meteorology and ice conditions from the U.S. National Ice Center. Results show the MRW ice forecasts in the Great Lakes outperform persistence-based forecasts. These findings could inform the development or extension of lake operational ice forecasting and the potential of coupling between atmospheric and large lake models at medium-range forecast time scales.

Plain Language Summary Ice information for large lakes is critical for essential operations, such as ice breaking, commercial navigation, search and rescue, and oil spill response. Ice forecasts are currently not available in the medium-range (5–16 days out) time scale, yet they could provide valuable information for decision making. This information could also be important for medium-range weather forecasts. The skill of existing Great Lakes ice forecast products at medium-range time scales is currently unknown. Our work aims to determine how well ice forecasts from an atmosphere-lake model perform for medium-range time scales. Simulations were carried out for the 2022 Great Lakes ice season, using 8 different 16-day forecast periods. The modeled forecasts were compared to observations from the National Ice Center and observed meteorological conditions. Results show that the modeled forecasts outperform persistence forecasts. These findings could inform the development or extension of ice forecasting and the potential of an atmosphere-lake model at medium-range time scales.

Key Points:

- Medium-range (5- to 16-day) ice forecasts show utility in the Great Lakes
- Model ice forecasts outperform ice persistence forecasts
- Air temperature bias in medium-range weather forecasts is the likely greatest contributor to ice error

Correspondence to:
A. J. Yeo,
alexayeo@mines.edu

Citation:
Yeo, A. J., Anderson, E. J., Jablonowski, C., Wright, D. M., Mann, G. E., Fujisaki-Manome, A., et al. (2024). Assessing the potential for medium-range ice forecasts in the Laurentian Great Lakes. *Water Resources Research*, *60*, e2024WR037507. https://doi.org/10.1029/2024WR037507

Received 12 MAR 2024
Accepted 12 AUG 2024

1. Introduction

The physical environment of lakes is a critical component to overall lake ecosystem function. Specifically, the hydrodynamic and ice environment of lakes are particularly important to ecosystem services like recreation, drinking water supply, and commercial use (Brammer et al., 2015; Hori et al., 2018; Hoyer et al., 2015). In recent years, most studies of lake ice have focused on ice phenology, or the dates of ice-on and -off, including the analysis of observed changes in global lake ice and projected conditions over the next century (Brown & Duguay, 2010; Huang et al., 2022; Magnuson et al., 2000; Sharma et al., 2019, 2021, 2022). However, in large lakes, which hold approximately 84% of Earth's surface freshwater (Anderson et al., 2021), the hydrodynamic-ice environment can be much more dynamic than in smaller lakes. While ice-on and -off dates remain important in large lakes, the daily variability in ice concentration and thickness introduces a different dimension in terms of stakeholder use and water management. Modeling these ice processes for historic simulation or forecasting purposes generally requires complex three-dimensional approaches, which have been studied in many applications in the Laurentian Great Lakes (e.g., Anderson et al., 2018).

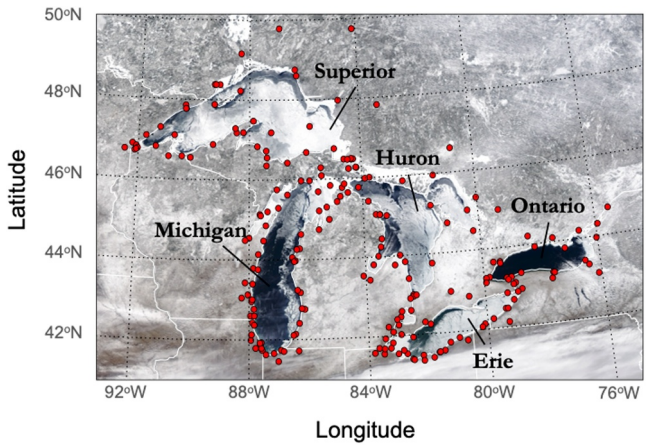

Figure 1. MODIS satellite image of the Laurentian Great Lakes under partial ice cover with coastal meteorological stations shown in filled red circles.

The Laurentian Great Lakes, hereafter the Great Lakes, contain five of the largest lakes on Earth that hold approximately 21% of the planet's surface freshwater supply, support more than $8.8 billion in wages in the maritime economic sector alone, and exhibit complex hydrodynamic processes including dynamic ice coverage in the winter season (NOAA; Figure 1). The entire basin spans the international border between the United States (US) and Canada, supporting several major cities, in which the US region alone has a gross domestic product of $3.1 trillion and employs more than 25 million people (NOAA). To support regional stakeholders in the protection of life and property, Great Lakes forecasting has been of interest for several decades. The earliest predictive models in routine operation for the Great Lakes were implemented by the National Oceanic and Atmospheric Administration (NOAA) National Weather Service (NWS) and provided the public with forecasts of dangerous water levels (Platzman, 1965; Schwab, 1978) and wind-waves (Schwab et al., 1984).

With the improvement of computational resources, predictive circulation models were developed for the Great Lakes and other coastal areas in a second wave of operational implementation. The first of its kind was the Great Lakes Forecast System (later, the Great Lakes Coastal Forecasting System), which combined a circulation model with sufficient meteorological observations in an operational framework that could support routine forecasts (Schwab & Bedford, 1994). These models were transitioned to NOAA operations in the early 2000s by the National Ocean Service (NOS; Great Lakes Operational Forecast System; Chu et al., 2007) and have since produced short-range forecasts of water levels, currents, and temperatures for 2-day and eventually 5-day time horizons.

More recently, attention has been paid to couple the hydrodynamic forecast system with an ice prediction capability in order to more thoroughly support stakeholder needs throughout the winter. Ice formation in the Great Lakes starts in late November or December and generally extends into April or even May, with significant spatial and interannual variation. In most years, Lakes Superior, Michigan, Huron, and Ontario do not completely freeze over, and ice is generally bound to coastal areas, bays, and other shallow regions, with the extent of lake-wide coverage driven by the intensity of the winter. Lake Erie is the exception, being the shallowest of the Great Lakes, and has seen annual maximum ice concentrations greater than 80% in 39 out the last 51 years (https://www.glerl.noaa.gov/data/ice/#historical). However, climate change has driven increases in regional air temperatures, solar radiation, and overwater wind speeds in recent decades (Anderson et al., 2021), all of which have led to decreasing trends in Great Lakes ice (Ozersky et al., 2021; Wang et al., 2018).

Over time, the Great Lakes have experienced fewer days of ice coverage, later ice-on dates and earlier ice-off dates, as well as decreased ice concentrations (Figure 2). Generally, these changes in ice conditions increase the potential days for commercial shipping and Coast Guard ice breaking activities in support of maritime transport. Furthermore, Great Lakes ice conditions can have a significant impact on regional weather forecasts through modification of turbulent surface fluxes of heat and moisture. Under certain conditions, openings in the ice can lead to extreme lake-effect precipitation events that can cause disruptions to ground transportation, aviation, municipal operations, and even injury or death (Fujisaki-Manome et al., 2017). For these reasons, accurate ice prediction has been identified as a critical requirement for Great Lakes stakeholders.

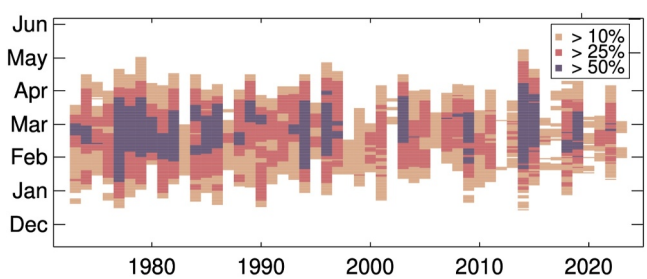

Figure 2. Historical Great Lakes basin wide ice concentration plotted for days with values greater than 10%, 25%, and 50% from 1973–2023 (adapted from Lenters et al., 2013).

Although ice modeling efforts were made much earlier (Wake & Rumer, 1979, p. 1983; Rumer et al., 1981), a coupled hydrodynamic-ice forecast system for the Great Lakes was not introduced until 2010 (Wang et al., 2010). As an update to the NOAA Great Lakes Coastal Forecast System (GLCFS), the Coupled Ice-Ocean Model (CIOM; Yao et al., 2000; Wang et al., 2010) was coupled with the underlying hydrodynamic model based on the Princeton Ocean Model (POM; Schwab & Bedford, 1994). Using this configuration, 5-day forecasts were generated by initializing the ice fields from satellite-derived concentrations from the U.S. National Ice Center and atmospheric forcing was supplied by the NOAA National Digital Forecast

Database (NDFD) to simulate hourly predictions of ice concentration, thickness, and velocity. Environment and Climate Change Canada (ECCC) also developed an ice prediction capability using the Nucleus for European Modeling of the Ocean model (NEMO; Dupont et al., 2012) and Los Alamos Sea Ice model (CICE; Hunke et al., 2017) as part of their Water Cycle Prediction System Coupled over the Great Lakes (WCPS-CGL; Dunford et al., 2018), which produces twice daily 3.5-day forecasts of lake and ice conditions.

Most recently, the NOAA Great Lakes Coastal Forecast System (GLCFS) was updated using the Finite Volume Community Ocean Model (FVCOM; Anderson et al., 2018; Chen et al., 2006). The FVCOM model includes an internally coupled unstructured version of the Los Alamos Sea Ice Model (CICE), which has been adapted for freshwater applications in the Great Lakes (Anderson et al., 2018; Bai et al., 2013, 2020; Cannon et al., 2024; Fujisaki-Manome et al., 2020; Kayastha et al., 2023; Lin et al., 2022). Beyond the upgrade of the base modeling system, the newest version of the GLCFS also began using weather forecast information from the NOAA High-Resolution Rapid Refresh (HRRR; Benjamin et al., 2016). The HRRR is a 3-km data-assimilated implementation of the Weather Research and Forecasting (WRF; Skamarock et al., 2008) model, which supplies the GLCFS with hourly surface forcing out to 48 hr. In NOAA operations, the remainder of the forecast period (48–120 hr) is driven by the NOAA National Digital Forecast Database (NDFD).

While short-range forecasts of lake and ice conditions have shown useful skill for many stakeholder needs (Fujisaki-Manome et al., 2019), commercial navigational planning, ice cutting operations, and weather forecasts all depend on conditions beyond the 5-day forecast horizon. However, the performance of large lake hydrodynamic-ice forecast models beyond short-range time scales has not been assessed. In this study, we aim to evaluate the potential of medium-range ice forecasts out to 16 days using operational products, and therefore we have chosen to use the coupled three-dimensional hydrodynamic-ice model employed operationally in the GLCFS for the Great Lakes. Specifically, we evaluate the potential for ice prediction at these time horizons using atmospheric forcing from the NOAA Global Forecast System (GFS; https://www.ncei.noaa.gov/products/weather-climate-models/global-forecast) that is supplied to a research version of the GLCFS. Overall, the aim is to assess the utility of medium-range ice forecasts for Earth's largest lakes using existing community models and operational products, derive insight into the deficiencies of ice prediction at these time scales, and determine where future effort should be spent to improve extended large lake ice forecasts.

2. Data and Methods

2.1. Atmospheric Modeling

In order to test medium-range ice forecast utility, atmospheric forcing data was acquired from the Global Forecast System (GFS) for the simulation periods described in Section 2.4. The NOAA GFS is a real-time operational forecast system that consists of coupled weather, ocean, land surface, and ice models that provide forecasted atmospheric conditions for the entire planet out to 384 hr, or 16 days. The GFS is updated every 6 hr at 00, 06, 12, and 18 UTC, producing hourly forecasts out to 120 hr, and 3-hourly forecasts from 120 to 384 hr. In the interest of characterizing GFS skill over the Great Lakes region during the ice season, we chose to compare meteorological observations (Section 2.3) to (a) GFS forecast data (hours 0 to 384, i.e. f000 to f384) and to (b) a baseline case (hereafter, analysis). The latter of which is a concatenation of the forecast hour zeros (f000) from the 6-hourly GFS cycles during each simulation period. The intent of the analysis case is to determine a best-case-scenario accuracy of the GFS model configuration as a point of comparison for the forecasted GFS meteorology, and it follows the common approach for creating a nowcast atmospheric forcing data set. It is reasonable to assume that hour zero (f000) of the GFS forecast would have the greatest accuracy compared to the subsequent forecast hours because it is closest in time to the initialization from observed data using the Global Data Assimilation Scheme v16 (GDAS; Kleist et al., 2009). More information on the GDAS process and GFS initialization is available from NOAA (https://www.ncei.noaa.gov/products/weather-climate-models/global-data-assimilation; https://www.emc.ncep.noaa.gov/emc/pages/numerical_forecast_systems/ncep_data_assimilation.php). In both cases, analysis and forecast, parameters for meteorological skill assessment and hydrodynamic-ice model forcing were acquired for the simulation periods described below, namely, zonal (east-west) and meridional (north-south) of wind velocity at 10-m height, air temperature and dewpoint temperature at 2-m height, total cloud cover, mean sea-level air pressure, specific humidity at 2-m height, and shortwave and longwave radiation.

2.2. Hydrodynamic-Ice Modeling

The hydrodynamic-ice model employed in this study is a research version of the NOAA GLCFS (Anderson et al., 2018). As described above, the GLCFS is based on coupled versions of FVCOM and CICE. FVCOM version 4.3.1 is a three-dimensional hydrodynamic model that solves the governing equations on an unstructured, terrain-following (sigma coordinate) grid and has been adapted for freshwater implementation. In its GLCFS implementation, FVCOM is configured with the Smagorinsky horizontal diffusion parameterization and Mellor-Yamada level 2.5 vertical turbulence closure schemes (Mellor & Yamada, 1982; Smagorinsky, 1963). Vertical and horizontal Prandtl numbers are set to 1.0. Turbulent heat fluxes for water portions of model elements are calculated using the wind-speed parameterization formulation of the Coupled Ocean-Atmosphere Response Experiment algorithm (COARE; Fairall et al., 2003). For ice-covered elements, the CICE model within FVCOM solves equations for ice thermodynamics and dynamics using an elastic-viscous-plastic (EVP) rheology to generate fields of ice concentration (e.g., coverage) and thickness. CICE uses a five-category ice thickness distribution (prescribed for the Great Lakes as 5, 25, 65, 125, and 205 cm) to handle ice growth, melting, and deformation. Turbulent heat fluxes over the ice are computed using bulk formations for (a) sensible, F_s, and (b) latent, F_l, heat flux components in the form,

$$F_s = \rho_a c_p u^* c_\theta (\Theta_a - T_{sf}) \quad (1)$$

$$F_l = \rho_a (L_{vap} + L_{ice})\, u^* c_q (Q_a - Q_{sf}) \quad (2)$$

where ρ_a is air density, c_p is specific heat, u^* is turbulent wind scale, c_θ and c_q are exchange coefficients, L_{vap} and L_{ice} are latent heats of vapourization and fusion, Θ_a is potential air temperature, T_{sf} is surface temperature, Q_a is the specific humidity, and Q_{sf} is the surface saturation specific humidity. Heat fluxes over fractional ice-covered cells are weighted by the ice area fraction, a_i, such that the flux, F, is computed by $F = a_i F_{ice} + (1-a_i)F_{water}$.

The GLCFS consists of four separate model domains that cover Lake Superior, Lake Erie, Lake Ontario, and a combined Lake Michigan-Huron. The unstructured grids range in resolution from 30 m near the coastline, or other topographically complex regions, to 3 km in offshore areas. All four models use a sigma vertical coordinate system with 21 uniformly distributed layers. For simplicity, this study did not prescribe lateral boundary conditions for river inflows or outflows. For each simulation period described in Section 2.4, lake conditions were initialized from real-time nowcast output from the GLCFS operated by NOAA, which included lake levels, three-dimensional currents and temperatures, ice conditions, and other parameters. It should be noted that the GLCFS nowcasts are driven by HRRR atmospheric forcing, not the GFS, which contains its own bias. Therefore, in order to independently assess the utility of GFS-driven medium-range forecasts and not include cumulative bias in the GLCFS, we adjusted the initial (i.e., hour 00 UTC) model water temperatures and ice conditions for each simulation using satellite-derived values of lake surface temperature and ice from the NOAA Great Lakes Surface Environmental Analysis (GLSEA; Schwab et al., 1999) and the U.S. National Ice Center (NIC), described in Section 2.3. In each case, the observed surface temperature from the GLSEA product was imparted on the model over the depth of the mixed layer and the ice conditions were updated from the NIC. While the GLSEA and NIC are daily products and not necessarily valid at hour 00 UTC (model start time), it provided the best approach for reducing potential cumulative bias present in the operational output.

In all simulations, the atmospheric forcing variables were spatially interpolated from the native 0.25-degree GFS to the FVCOM grids for each lake within the GLCFS. The required atmospheric forcing for FVCOM-CICE includes 10-m wind, shortwave and longwave radiation, 2-m air and dewpoint temperatures, mean sea-level pressure, and 2-m specific humidity. Analysis and forecast simulations in FVCOM-CICE had identical configurations with the exception of differences in time-interval between the analysis (f000; 6-hourly for 0–384 hr) and forecast forcing (hourly for 0–120 hr, 3-hourly for 120–384 hr). In both cases, the atmospheric forcing was linear-interpolated between time stamps, which is the default FVCOM methodology.

2.3. Ice and Meteorological Data

Daily charts of ice concentration in the Great Lakes were acquired through a collaboration between the U.S. National Ice Center (US NIC) and the Canadian Ice Service (Figure 3). The ice data, hereafter referred to as the NIC, are derived from available satellite remote sensing (e.g., MODIS, GOES, AVHRR, Radarsat-2, Envisat) and

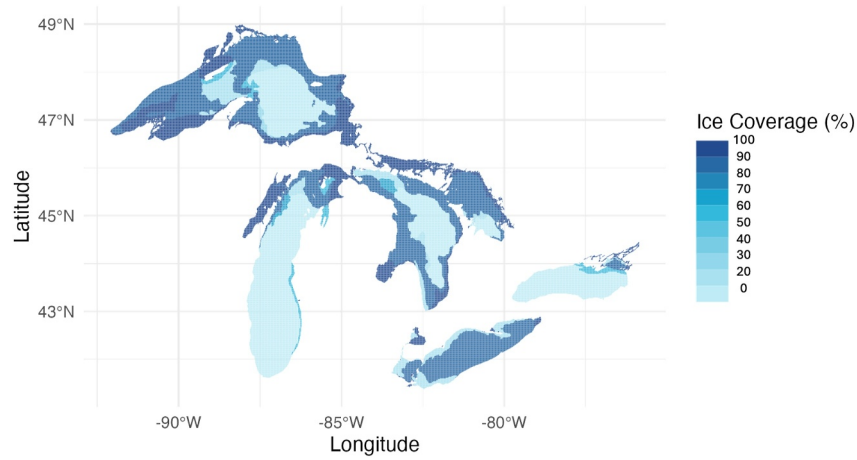

Figure 3. Example of US NIC ice chart data depicting spatial distribution of ice concentration categories for 3 March 2022. Data is given in 10% increments with bins for the values of 0%, 20%, 30%, 40%, 50%, 60%, 70%, 80%, 90%, and 100%.

provided on 1.8 km grid over the Great Lakes by the NOAA Coastwatch program (https://coastwatch.glerl.noaa.gov/). Gridded concentrations are given in 10% increments from 0% to 100% coverage and while a valid date is given for each day, the concentrations on a given day may be an amalgam of previous days' satellite observations or other reports. Therefore, it is considered that the US NIC data provide a reasonable representation of ice conditions and changes throughout the season but may not reflect the true state of the ice field for a particular day. Nevertheless, the US NIC data are the best source for daily fields of ice concentration for the Great Lakes. In addition to ice conditions, surface water temperatures for model initialization and validation were acquired from the NOAA GLSEA (Schwab et al., 1999). The GLSEA provides gridded daily surface temperatures for all of the Great Lakes based on observations from the Advanced Clear-sky Processor for Oceans L3S-LEO SST, which is level 3 Super Collated data from various satellites (e.g., NPP, N20, MetOp A/B/C).

To assess the accuracy of atmospheric forcing, meteorological observations were acquired for the Great Lakes region using a subset of stations ($n = 218$) that lie near (or on) the water and that have historically been used for lake analyses and hydrodynamic simulation (Schwab & Bedford, 1994; https://apps.glerl.noaa.gov/marobs/; Figure 1). This network of stations consists of data from the NOAA Coastal-Marine Automated Network (C-MAN), Automated Surface Observing System (ASOS), National Data Buoy Center (NDBC), and the Real-time Coastal Observing Network (ReCON) from the NOAA Great Lakes Environmental Research Laboratory. Observed parameters of wind speed, air temperature, dewpoint temperature, and cloud cover were compared to the atmospheric model. Adjustments of the observed data were made to standard 10-m height for wind speed and 2-m height for air temperature and dewpoint temperature by accounting for atmospheric stability (Schwab & Bedford, 1994). For each station, GFS data were filtered by a land/water mask (e.g., land points used for land stations, water points for lighthouses/buoys) and interpolated to the station locations using a nearest neighbor method. Atmospheric model skill was assessed using root-mean square error (RMSE) and bias for individual stations (across the simulation period) and by forecast day (across all stations).

2.4. Forecast Scenarios and Validation

Simulations were carried out for 8 forecast periods in 2022, starting on the first and fifteenth of each month and running for 16 days. The year 2022 (Figure 4) was chosen because it overlapped with available GFS v16 data and is representative of long term average ice concentrations. For instance, the basin-wide average ice concentration in 2022 was 56.1% as compared to the long term basin-wide average ice concentration of 52% (Data from NOAA: https://www.glerl.noaa.gov/data/ice/glicd/AMIC.txt). The simulation periods are as follows: January 1–16, January 15–30, February 1–16, February 15–March 3, March 1–16, March 15–30, April 1–16, and April 15–30. Observations from the US NIC were compared to model simulations as driven by the GFS forecast and the analysis scenarios. With 8 simulation periods, 4 model domains, and 2 forcings (forecast and analysis), there were a total of 64 simulations carried out for this study. US NIC and modeled ice was also compared to an ice persistence forecast, where day 1 ice conditions from the US NIC are kept constant over the 16-day period. Model

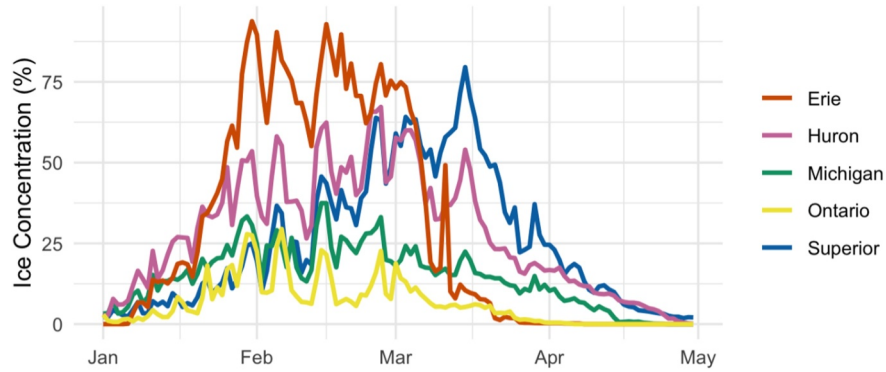

Figure 4. Lake-average ice concentration time-series from US NIC for January–May 2022.

skill was assessed using RMSE and bias calculated for each day of the forecast period in each simulation and RMSE plotted spatially over the FVCOM grid on each lake. Finally, while not a direct comparable to medium-range prediction, archived ice forecasts from the short-range GLCFS were acquired and used to calculate a short-range RMSE as a benchmark for comparison. Archives of short-range GLCFS ice are only available out to day 3 of the forecast, and thus they were used to provide the benchmark RMSE.

3. Results and Discussion

3.1. GFS Baseline and Forecast Skill

Wind-speed, air temperature, dewpoint temperature, and cloud cover are the common atmospheric parameters measured at the meteorological stations, available in the GFS, and supplied to the hydrodynamic-ice model. For all matching timestamps, the GFS variables were compared to the available meteorological observations for the entire simulation period (e.g., January through April 2022). Station-based comparisons of the analysis GFS (forecast hour zero; f000) reveal notable bias across all four variables (Figure 5). In general, air temperature, dewpoint temperature, and wind speed are low-biased at a majority of the stations (Figures 5a–5c and 5d). Analysis cloud cover is high-biased at most stations (Figure 5b), which means a low-bias in solar radiation input to the lakes. Analysis air temperatures show a north-south gradient in air temperature bias, with the greatest negative bias found around Lake Superior and the smallest biases located at the southern ends of Lake Michigan and Lake Erie. In all, baseline comparisons for the analysis suggest that at forecast hour zero the GFS atmospheric forcing is prone to result in cold biased lake water temperatures and the potential for greater ice conditions than would be observed.

Forecasted atmospheric conditions from the GFS reveal a similar bias when compared to station observations (Figure 6). When the GFS is evaluated across all eight of the 16-day forecast periods, a north-south gradient in air temperature bias is apparent and similar to the baseline comparisons, with forecast temperatures near Lake Superior have the most significant low-bias (Figure 6a). Like the analysis evaluation, cloud cover high-bias and wind speed low-bias are prevalent at most stations (Figures 6b and d). Only in forecasted dewpoint temperatures is there a notable change from the baseline analysis, where a similar number of stations across the Great Lakes region reveal low- and high-biased values (Figure 6c). However, the high-biased station dewpoints tend to be found along the southern coast of Lake Erie, eastern coast of Lake Michigan, and the south-eastern portion of Lake Ontario. While each of these regions are generally downwind given the common weather patterns for the area, the same gradients are not found for Lakes Superior and Huron. Again, however, the mean bias across all stations for the GFS forecast suggest the potential for cold-biased lake temperatures or increased ice growth. Daily mean bias across all stations for each forecast day reveal GFS forecasted conditions behave similarly to the baseline conditions, with perhaps greater variability beyond day 7 (Figure 7). However, RMSE of the GFS forecasted parameters over the forecast period reveals a significant divergence from the analysis values in air and dewpoint temperatures after forecast day 10 and 16, respectively (Figures 7a and c).

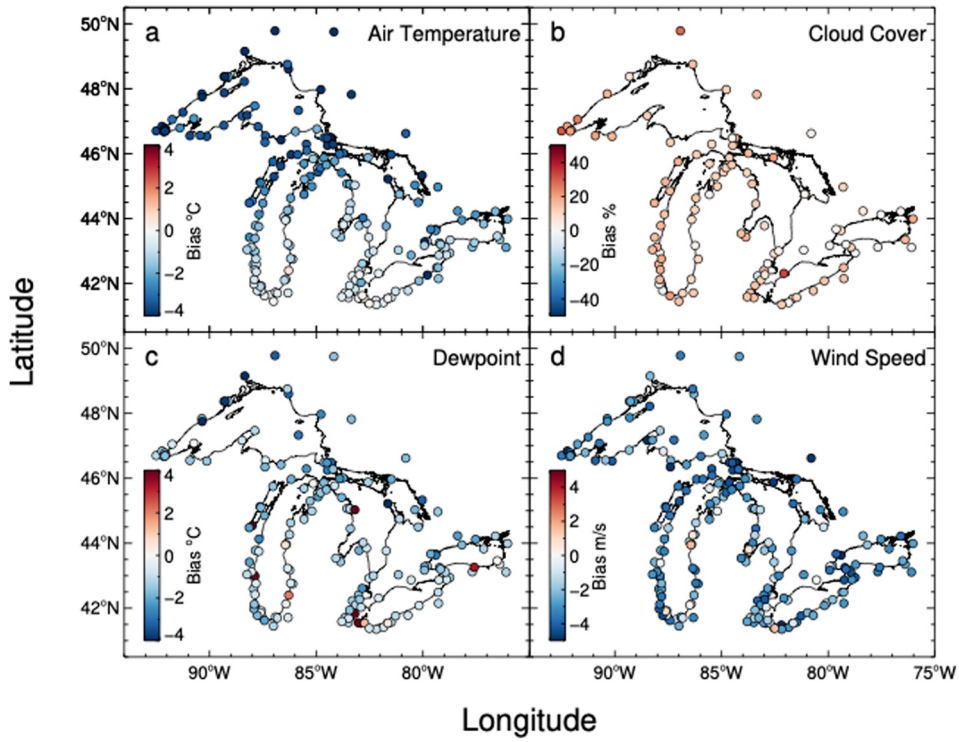

Figure 5. Mean bias between GFS analysis (forecast hour zero; f000) and meteorological observations for (a) air temperature, (b) cloud cover, (c) dewpoint, and (d) wind speed during the period January through April 2022.

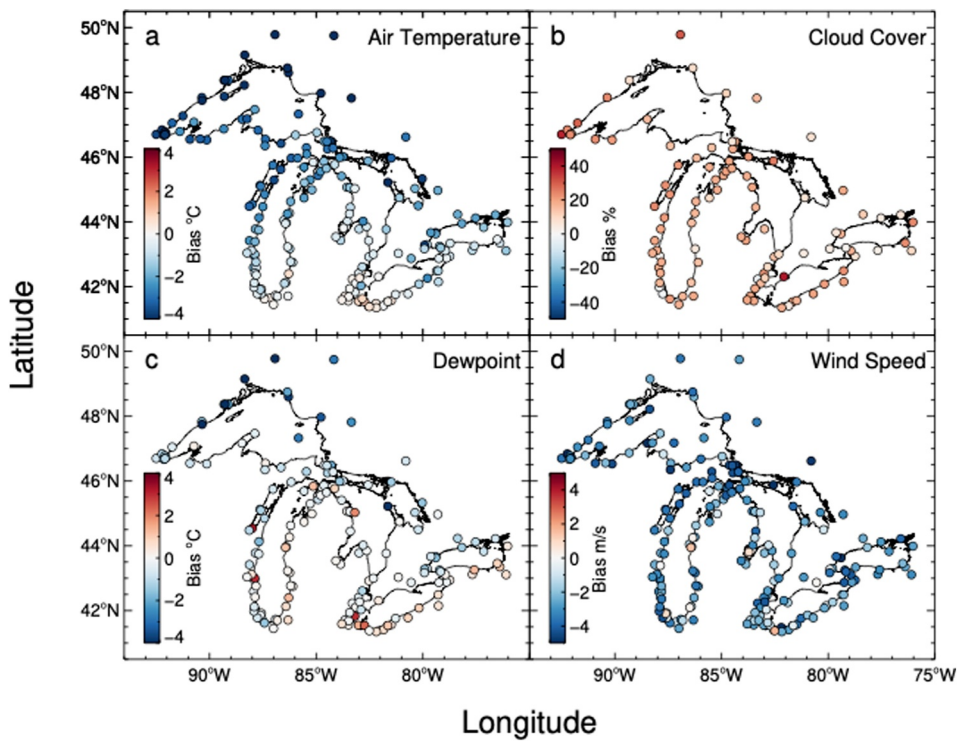

Figure 6. Mean bias between GFS forecast and meteorological observations for (a) air temperature, (b) cloud cover, (c) dewpoint, and (d) wind speed during the period January through April 2022.

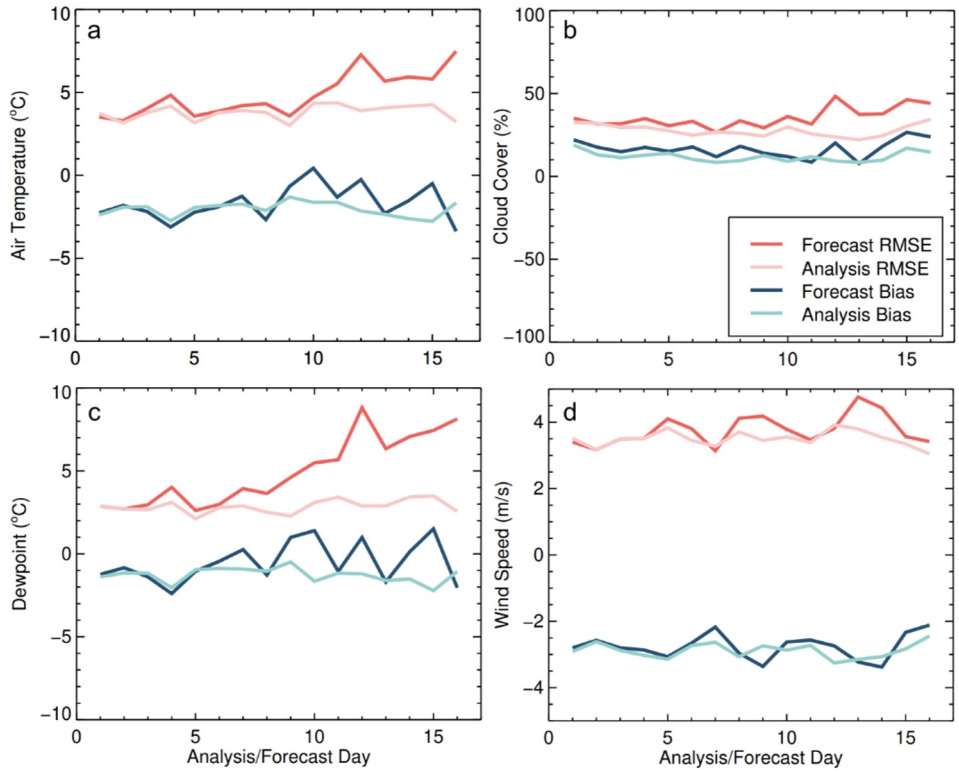

Figure 7. RMSE and mean bias of the GFS analysis (forecast hour zero; f000) on each day of simulation period (calculated across all simulations), and RMSE and mean bias of the forecast simulations (calculated as a function of forecast day across all simulations) across all stations for (a) air temperature, (b) cloud cover, (c) dewpoint, and (d) wind speed.

3.2. Lake Ice Skill

GLCFS ice forecasts under the two atmospheric forcings (GFS forecast and analysis) were compared to US NIC observations during eight time periods in 2022. Lake-averaged ice concentrations are plotted for NIC, model forecast and analysis, and persistence scenarios (Figure 8). In January, US NIC observations show that the lakes experience rapid ice growth, with Erie concentrations rising to 87% and the remaining lake concentrations ranging from 25% to 50% by the end of the month. Aside from the Jan 1 simulation period, the persistence forecast in this month significantly underpredicts ice concentrations. However, with the exception of Lake Superior, model forecasted ice concentrations during January agree well with the US NIC data. The analysis (or baseline) simulation, while generally following the observed and forecasted cases, overpredicts ice concentrations in the Jan 15 period, particularly for Lake Ontario (Figure 8d), Lake Huron (Figure 8b), and Lake Erie (Figure 8a).

In February, which is peak ice season for all but Lake Superior, the observed ice concentrations from US NIC reveal a high degree of variability over the 16-day periods. While the respective persistence forecasts are somewhat characteristic of the mean concentration over the time period, compared to January, by definition they cannot capture the large swings in observed concentrations. Forecast and analysis scenarios track the observed variability well for Lakes Michigan, Huron, and Ontario, whereas Lake Erie is a mixed result. In the February 1 simulations for Lake Erie (Figure 8a), forecast and analysis models overpredict ice concentrations compared to the observed concentrations and fail to resolve the fluctuations in ice around day-4 and -12. However, in the Feb 15 case, both simulations track the observed ice until day-8, at which the forecast simulation predicts an unrealistic drop in ice concentration, while the analysis continues to track the US NIC until at least day 12. Further inspection of the meteorology reveals the forecast for Lake Erie has an extreme high bias air temperature (~10°C; not shown) that is the driver behind the discrepancy.

In the receding limb of the ice season, the model forecast and analysis simulations generally capture the trend in observed ice. As would be expected during the melting season, the persistence forecast overpredicts ice conditions for most cases during this period except when there is very little change. While the forecast and analysis

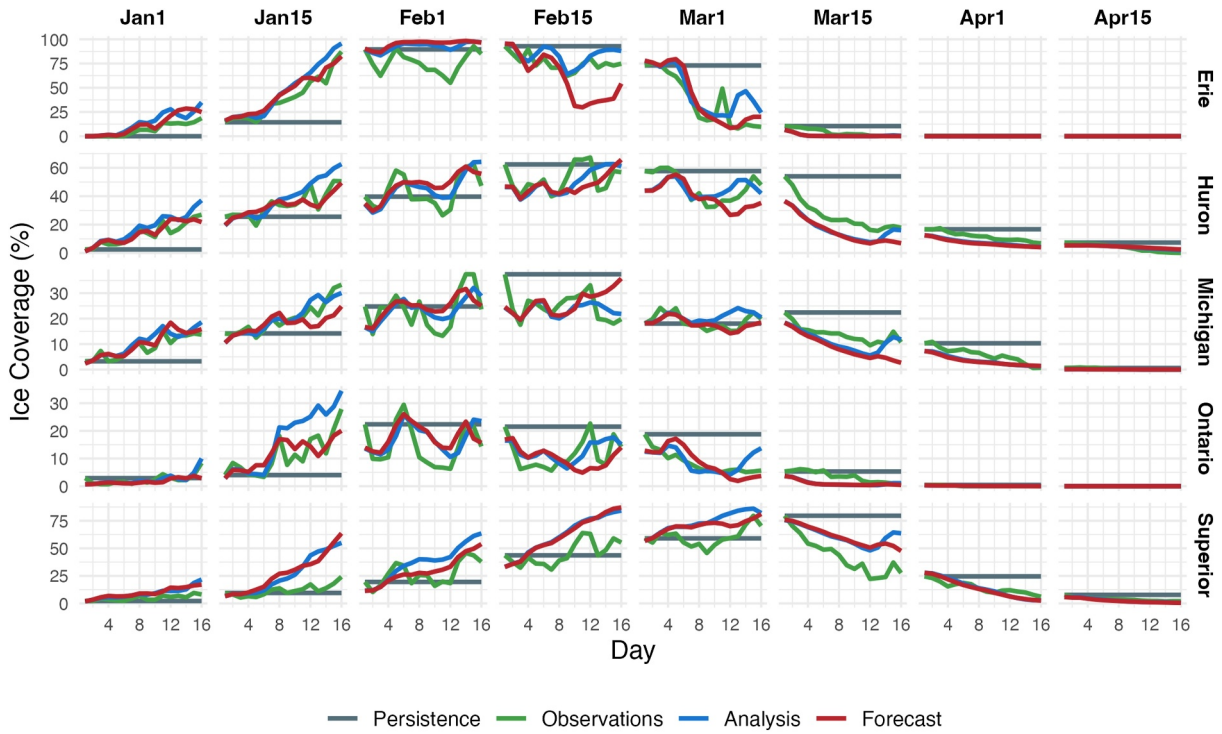

Figure 8. Ice coverage comparison of the forecast and analysis forcings, persistence, and observations for (a) Lake Erie, (b) Lake Huron, (c) Lake Michigan, (d) Lake Ontario, and (e) Lake Superior.

track the receding ice fields during these months, there is a noticeable bias in Huron, Michigan, and Superior during the Mar 15 simulation. While the meteorology is primarily responsible for these differences, day-1 bias may in fact stem from the ice initialization used in the model. As observations only include ice concentration, assumptions about ice thickness must be made for model initialization, which is also true for subsurface temperatures but less significant in this case.

Across most of the season, model predicted ice strays most from the US NIC data in Lake Superior. Generally, the simulated ice follows the trend of ice growth or melting observed during each case, but the ice initialization in the model also helps keep predictions close to realistic. In any case, even with the low-bias air temperatures identified over Lake Superior (Figures 5 and 6), the overprediction of ice is consistent with a shallow mixed layer present in the hydrodynamic-ice model, which has been identified previously (Kelley et al., 2022). The absence of a deeper mixed layer results in artificially cooler surface temperatures than observed and also the rapid growth of ice, which is present in most of the months. The deficiencies in the GFS forcing over Lake Superior are likely exacerbating this error.

Root Mean Squared Error (RMSE) and bias % of ice cover were calculated to quantify the model skill. For each lake, an overall RMSE value was calculated for each day of the forecast across all eight forecast periods. In all lakes, RMSE increased over the length of the forecast horizon, most notably in Erie and Superior (Figure 9). These RMSE values also align well with short-range ice forecasts on day 3 of the forecast period. In the simulated cases, day-1 RMSE may be a function of both the initialization limitations and actual ice variability driven by the GFS. In all lakes, the model forecast and analysis generally perform better than the persistence case. In Lakes Michigan, Huron, and Ontario, the ice RMSE stays below 10% for the entire 16-day range. In Lakes Michigan and Ontario, the persistence RMSE is roughly 5% higher than the modeled cases, though in Lake Huron, the persistence is as much as 10% greater. In Lake Erie, the modeled RMSE stays below 10% until day-8. For days 8–16, the analysis simulation stays below 20%, though the forecast RMSE jumps above 20% for day-10, likely due to the meteorological deficiency pointed out earlier. In comparison, the persistence forecast for Lake Erie steadily rises over the forecast duration to nearly 35% by day-16. In Lake Superior, each case sees a steady increase in RMSE over the forecast length, though the peak RMSEs are near 20%. In all cases, the forecast and analysis

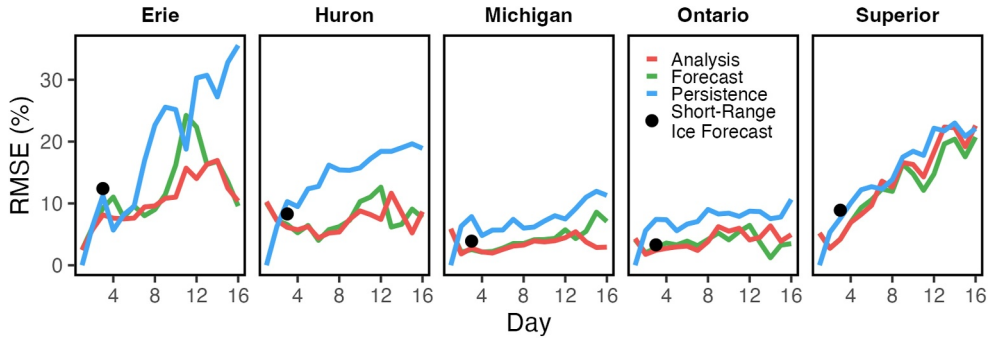

Figure 9. RMSE calculated for each day of each forecast period, shown for all five lakes along with the archived GLCFS short-range ice forecast RMSE at day 3 provided for reference.

simulations are generally similar. It is important to note that at some level the model RMSE is a function of the US NIC data precision. The US NIC data is only given in 10% increments, whereas the model is continuous, and thus the true model error is unclear at this resolution.

In addition to model skill across the forecast horizon, RMSE was also evaluated spatially across the lake surfaces, allowing for the determination of geographic patterns in model skill at different forecast horizons. For all forecast horizons, RMSE is generally higher in areas of high ice concentrations, which include bays, shallow regions, and coastlines, and lower in offshore regions (Figure 10). But particularly high RMSE values seem to align with areas that are both shallow and semi-enclosed. For example, Green Bay (approx. 87°W, 45°N) in Lake Michigan has an RMSE greater than 40% over most of the bay on days 5, 10, and 16 of the forecast period. However, we can see that this is not always the case, as Lake Erie RMSE on day-5 is below 10% for much of the central basin of Lake Erie, even though ice concentrations are high and depths are less than 19 m, and Saginaw Bay (approx. 83.5°W, 44.0°N) in Lake Huron, which is both shallow and semi-enclosed, has an RMSE between 15% and 30%. Therefore, additional factors might play an important role for Green Bay, such as hydrologic (river) inflows that could serve to enhance circulation and flush out the bay, or the air temperature bias observed over the higher latitudes of the region. On forecast day 10, the patterns of RMSE are similar but tend to increase in magnitude, with the exception of offshore Lake Michigan and Lake Huron and the majority of Lake Ontario (Figure 10b). Yet even on forecast day 16, with the exception of Lake Superior, patterns remain consistent but RMSE does not significantly increase (Figure 10c). In Lake Superior, most of the lake is between 30% and 60%, with no major distinctions between coastal and offshore regions. It is reasonable to assume that both the low-bias air temperatures in the GFS around Superior (Figure 6) and the general increase in air temperature RMSE after day 10 (Figure 7) contribute to this effect. Additionally, error could be exasperated by deficiencies in model physics. For example, insufficient mixing in deep lakes, such as Superior, or the lack of wave-ice interaction in lakes with large fetch could lead to overprediction of ice concentration and thickness. In all the patterns, and even magnitude of RMSE, are similar to values reported in the literature (Anderson et al., 2018), even at these medium-range forecast horizons. Although the usefulness of these forecasts for stakeholders would vary depending on their specific needs, ice concentration information was ranked as the second most important piece of information in decision-making for navigation and shipping sectors in the Great Lakes (Fujisaki-Manome et al., 2019). The model skill demonstrated here would offer additional planning and decision-making information to stakeholders beyond the 5-day time horizon.

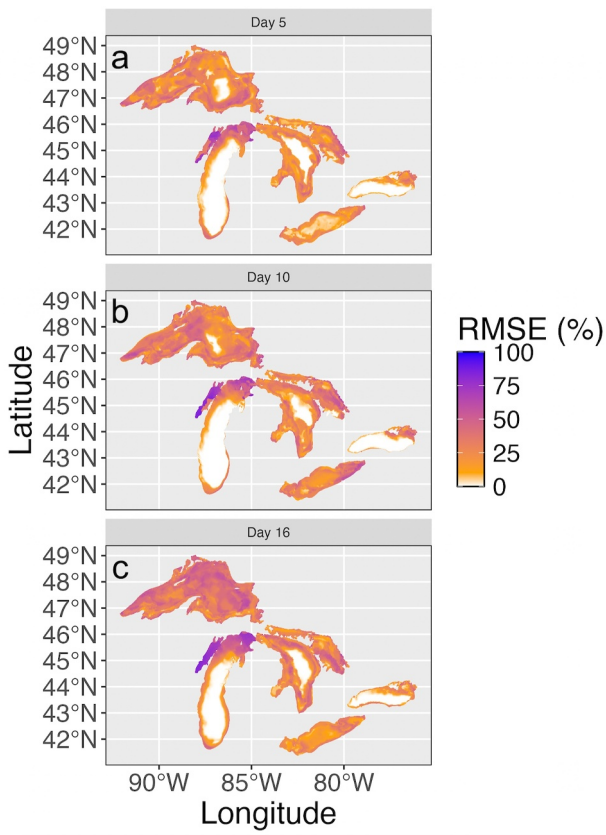

Figure 10. Spatial representation of RMSE for modeled forecast ice concentration on (a) day 5, (b) day 10, and (c) day 16, calculated across all simulations.

4. Conclusions

Ice forecasting in Earth's large lakes is relatively new compared to the long history of lake numerical modeling and operational prediction. While short-range predictions, which are typically 3 or 5 days forecast horizons, have been available for the Laurentian Great Lakes since 2010, no attempt has been made to assess the skill of medium-range ice forecasts in these large lakes. In this study, we use existing operational models to assess the utility of medium-range ice forecasts out to 16 days. This work shows that even with deficiencies in forecasted meteorological conditions at these time scales, medium-range ice prediction in the Great Lakes may have accuracy that meets stakeholder requirements for shipping, spill response, and ice cutting operations. In all cases, the model forecasts perform better than the persistence forecast. The success of this approach hinges upon reasonable starting conditions for the lake temperature and ice field. While existing nowcast operations have known bias in both of these respects, there have been advancements to better integrate remote sensing and data assimilation techniques into operational lake prediction. For medium-range forecasts such as those presented here, it is imperative that hydrodynamic-ice bias is minimized before initiating medium-range forecast simulation.

This work also reveals the potential for improvement to medium-range ice forecasts by improving the underlying operational lake and weather forecast models. For example, the shallow mixed layer present in the Great Lakes models inhibits vertical mixing, which in the winter time means that the surface artificially cools instead of bringing up relatively warm water from below. The result of this insufficient mixing is overgrowth of ice concentration and thickness that increases seasonal RMSE and inhibits melting in the spring season. However, other processes may also contribute to the overproduction of ice, including the lack of wave-ice interaction physics in the operational configuration.

In addition, while the GFS is a coarse-scale (0.25°) global weather model, the forecasted values in the Great Lakes region can yield useful ice predictions at medium-range time scales when the lake model is properly initialized. However, it is clear from the bias calculated for the analysis case that the assimilation scheme used to generate the hour-0 meteorology can be improved. It is reasonable to assume any reduction in atmospheric bias present in the air temperature, cloud cover, and wind, as reported here, would lead directly to improved medium-range ice prediction.

Overall, this work demonstrates the skill of medium-range ice prediction in the Great Lakes using existing operational and community models. While RMSE increases with increasing forecast horizon, the skill of ice prediction out to 10 days, and maybe further, can still be useful to many stakeholders and ecosystem services surrounding ice-covered large lakes. Though not explored here, the coupling of large lake models with weather forecast models over medium-range time scales may have the potential to improve synoptic weather forecasts in the Great Lakes region while also increasing ice forecast accuracy.

Data Availability Statement

All data used in this study are publicly available. The atmospheric data used from the GFS are available from https://www.ncei.noaa.gov/products/weather-climate-models/global-forecast, the FVCOM-CICE model is available from https://www.fvcom.org/, and the GLCFS data/configuration is available from https://www.ncei.noaa.gov/thredds/catalog/model/model.html. Surface temperature data used for model initialization are available from NOAA CoastWatch: https://coastwatch.glerl.noaa.gov/statistics/average-surface-water-temperature-glsea/. Great Lakes ice data are available from https://usicecenter.gov/. Meteorological data used for assessment of the GFS are available from NOAA: https://apps.glerl.noaa.gov/marobs/.

Acknowledgments
This work was funded by the National Oceanic and Atmospheric Administration's Weather Program Office Joint Technology Transfer Initiative awarded to the University of Michigan (NA22OAR4590188) and subaward to the Colorado School of Mines (SUBK00016687). This is GLERL contribution number 2056 and CIGLR contribution number 1248.

References

Anderson, E. J., Fujisaki-Manome, A., Kessler, J., Lang, G. A., Chu, P. Y., Kelley, J. G., et al. (2018). Ice forecasting in the next-generation great lakes operational forecast system (GLOFS). *Journal of Marine Science and Engineering*, *6*(4), 123. https://doi.org/10.3390/jmse6040123

Anderson, E. J., Stow, C. A., Gronewold, A. D., Mason, L. A., McCormick, M. J., Qian, S. S., et al. (2021). Seasonal overturn and stratification changes drive deep-water warming in one of Earth's largest lakes. *Nature Communications*, *12*(1), 1688. https://doi.org/10.1038/s41467-021-21971-1

Bai, P., Wang, J., Chu, P., Hawley, N., Fujisaki-Manome, A., Kessler, J., et al. (2020). Modeling the ice-attenuated waves in the great lakes. *Ocean Dynamics*, *70*(7), 991–1003. https://doi.org/10.1007/s10236-020-01379-z

Bai, X., Wang, J., Schwab, D. J., Yang, Y., Luo, L., Leshkevich, G. A., & Liu, S. (2013). Modeling 1993–2008 climatology of seasonal general circulation and thermal structure in the Great Lakes using FVCOM. *Ocean Modelling*, *65*, 40–63. https://doi.org/10.1016/j.ocemod.2013.02.003

Benjamin, S. G., Weygandt, S. S., Brown, J. M., Hu, M., Alexander, C. R., Smirnova, T. G., et al. (2016). A North American hourly assimilation and model forecast cycle: The Rapid Refresh. *Monthly Weather Review*, *144*(4), 1669–1694. https://doi.org/10.1175/mwr-d-15-0242.1

Brammer, J. R., Samson, J., & Humphries, M. M. (2015). Declining availability of outdoor skating in Canada. *Nature Climate Change*, *5*(1), 2–4. https://doi.org/10.1038/nclimate2465

Brown, L. C., & Duguay, C. R. (2010). The response and role of ice cover in lake-climate interactions. *Progress in Physical Geography*, *34*(5), 671–704. https://doi.org/10.1177/0309133310375653

Cannon, D., Wang, J., Fujisaki-Manome, A., Kessler, J., Ruberg, S., & Constant, S. (2024). Investigating multidecadal trends in ice cover and subsurface temperatures in the laurentian great lakes using a coupled hydrodynamic–ice model. *Journal of Climate*, *37*(4), 1249–1276. https://doi.org/10.1175/jcli-d-23-0092.1

Chen, C., Beardsley, R. C., & Cowles, G. (2006). Finite volume coastal ocean. *Oceanography*, *19*(1), 78–89. https://doi.org/10.5670/oceanog.2006.92

Chu, P., Kelley, J. G. W., Zhang, A. J., Lang, G. A., & Bedford, K. W. (2007). Skill assessment of NOS Lake Erie operational forecast system (LEOFS). *NOAA Technical Memorandum NOS CS*, *12*.

Dupont, F., Chittibabu, P., Fortin, V., Rao, Y. R., & Lu, Y. (2012). Assessment of a NEMO-based hydrodynamic modelling system for the Great Lakes. *Water Quality Research Journal of Canada*, *47*(3–4), 198–214. https://doi.org/10.2166/wqrjc.2012.014

Durnford, D., Fortin, V., Smith, G. C., Archambault, B., Deacu, D., Dupont, F., et al. (2018). Toward an operational water cycle prediction system for the Great Lakes and St. Lawrence River. *Bulletin of the American Meteorological Society*, *99*(3), 521–546. https://doi.org/10.1175/bams-d-16-0155.1

Fairall, C. W., Bradley, E. F., Hare, J. E., Grachev, A. A., & Edson, J. B. (2003). Bulk parameterization of air–sea fluxes: Updates and verification for the COARE algorithm. *Journal of Climate*, *16*(4), 571–591. https://doi.org/10.1175/1520-0442(2003)016<0571:bpoasf>2.0.co;2

Fujisaki-Manome, A., Anderson, E. J., Kessler, J. A., Chu, P. Y., Wang, J., & Gronewold, A. D. (2020). Simulating impacts of precipitation on ice cover and surface water temperature across large lakes. *Journal of Geophysical Research: Oceans*, *125*(5), e2019JC015950. https://doi.org/10.1029/2019jc015950

Fujisaki-Manome, A., Fitzpatrick, L. E., Gronewold, A. D., Anderson, E. J., Lofgren, B. M., Spence, C., et al. (2017). Turbulent heat fluxes during an extreme lake-effect snow event. *Journal of Hydrometeorology*, *18*(12), 3145–3163. https://doi.org/10.1175/jhm-d-17-0062.1

Fujisaki-Manome, A., Gill, D. G., Anderson, E. J., Guo, T., & Lemos, M. C. (2019). *Report on the Great lakes ice forecast workshop*. Available from the University of Michigan Graham Sustainability Institute web site. Retrieved from http://graham.umich.edu/activity/43899

Hori, Y., Cheng, V. Y., Gough, W. A., Jien, J. Y., & Tsuji, L. J. (2018). Implications of projected climate change on winter road systems in Ontario's Far North, Canada. *Climatic Change*, *148*(1–2), 109–122. https://doi.org/10.1007/s10584-018-2178-2

Hoyer, A. B., Schladow, S. G., & Rueda, F. J. (2015). A hydrodynamics-based approach to evaluating the risk of waterborne pathogens entering drinking water intakes in a large, stratified lake. *Water Research*, *83*, 227–236. https://doi.org/10.1016/j.watres.2015.06.014

Huang, L., Timmermann, A., Lee, S. S., Rodgers, K. B., Yamaguchi, R., & Chung, E. S. (2022). Emerging unprecedented lake ice loss in climate change projections. *Nature Communications*, *13*(1), 5798. https://doi.org/10.1038/s41467-022-33495-3

Hunke, E., Lipscomb, W., Jones, P., Turner, A., Jeffery, N., & Elliott, S. (2017). *CICE, the Los Alamos sea ice model (No. CICE; 005315WKSTN00)*. Los Alamos National Laboratory (LANL).

Kayastha, M. B., Huang, C., Wang, J., Pringle, W. J., Chakraborty, T. C., Yang, Z., et al. (2023). Insights on simulating summer warming of the great lakes: Understanding the behavior of a newly developed coupled lake-atmosphere modeling system. *Journal of Advances in Modeling Earth Systems*, *15*(7), e2023MS003620. https://doi.org/10.1029/2023ms003620

Kelley, J. G. W., Chen, Y., Anderson, E. J., Lang, G. A., & Peng, M. (2022). Upgrade of NOS Lake Superior operational forecast system to FVCOM: Model development and hindcast skill assessment. *NOAA technical memorandum NOS CS*, *48*.

Kleist, D. T., Parrish, D. F., Derber, J. C., Treadon, R., Wu, W. S., & Lord, S. (2009). Introduction of the GSI into the NCEP global data assimilation system. *Weather and Forecasting*, *24*(6), 1691–1705. https://doi.org/10.1175/2009waf2222201.1

Lenters, J. D., Anderton, J. B., Blanken, P., Spence, C., & Suyker, A. E. (2013). Assessing the impacts of climate variability and change on great lakes evaporation. In D. Brown, D. Bidwell, & L. Briley (Eds.), *Available from the Great lakes integrated sciences and assessments (GLISA) center. 2011 project reports* Retrieved from http://glisaclimate.org/media/GLISA_Lake_Evaporation.pdf

Lin, Y., Fujisaki-Manome, A., & Anderson, E. J. (2022). Simulating landfast ice in Lake Superior. *Journal of Marine Science and Engineering*, *10*(7), 932. https://doi.org/10.3390/jmse10070932

Magnuson, J. J., Robertson, D. M., Benson, B. J., Wynne, R. H., Livingstone, D. M., Arai, T., et al. (2000). Historical trends in lake and river ice cover in the Northern Hemisphere. *Science*, *289*(5485), 1743–1746. https://doi.org/10.1126/science.289.5485.1743

Mellor, G. L., & Yamada, T. (1982). Development of a turbulence closure model for geophysical fluid problems. *Reviews of Geophysics*, *20*(4), 851–875. https://doi.org/10.1029/rg020i004p00851

National Oceanic and Atmospheric Administration (NOAA). Based on data from the Bureau of labor statistics and the Bureau of economic analysis economics: National ocean watch (ENOW) data. NOAA Office for Coastal Management.

Ozersky, T., Bramburger, A. J., Elgin, A. K., Vanderploeg, H. A., Wang, J., Austin, J. A., et al. (2021). The changing face of winter: Lessons and questions from the Laurentian Great Lakes. *Journal of Geophysical Research: Biogeosciences*, *126*(6). https://doi.org/10.1029/2021jg006247

Platzman, G. W. (1965). The prediction of surges in the southern basin of Lake Michigan: Part I. The dynamical basis for prediction. *Monthly Weather Review*, *93*(5), 275–281. https://doi.org/10.1175/1520-0493(1965)093<0275:tposit>2.3.co;2

Rumer, R. R., Wake, A., & Chieh, S. H. (1981). Development of an ice dynamics forecasting model for Lake Erie. *Department of Civil Engineering and Center for Cold Regions Engineering, Science and Technology, State University of New York at Buffalo*.

Schwab, D. J. (1978). Simulation and forecasting of Lake Erie storm surges. *Monthly Weather Review*, *106*(10), 1476–1487. https://doi.org/10.1175/1520-0493(1978)106<1476:safole>2.0.co;2

Schwab, D. J., & Bedford, K. W. (1994). Initial implementation of the great lakes forecasting system: A real-time system for predicting lake circulation and thermal structure. *Water Pollution Research Journal of Canada*, *29*(2and3), 203–220. https://doi.org/10.2166/wqrj.1994.014

Schwab, D. J., Leshkevich, G. A., & Muhr, G. C. (1999). Automated mapping of surface water temperature in the Great Lakes. *Journal of Great Lakes Research*, *25*(3), 468–481. https://doi.org/10.1016/s0380-1330(99)70755-0

Schwab, D. J., Meadows, G. A., Bennett, J. R., Scnultz, H., Liu, P. C., Campbell, J. E., & Dannelongue, H. H. (1984). The response of the coastal boundary layer to wind and waves: Analysis of an experiment in Lake Erie. *Journal of Geophysical Research*, *89*(C5), 8043–8053. https://doi.org/10.1029/jc089ic05p08043

Sharma, S., Blagrave, K., Filazzola, A., Imrit, M. A., & Hendricks Franssen, H. J. (2021). Forecasting the permanent loss of lake ice in the Northern Hemisphere within the 21st century. *Geophysical Research Letters*, *48*(1), e2020GL091108. https://doi.org/10.1029/2020gl091108

Sharma, S., Blagrave, K., Magnuson, J. J., O'Reilly, C. M., Oliver, S., Batt, R. D., et al. (2019). Widespread loss of lake ice around the Northern Hemisphere in a warming world. *Nature Climate Change*, *9*(3), 227–231. https://doi.org/10.1038/s41558-018-0393-5

Sharma, S., Filazzola, A., Nguyen, T., Imrit, M. A., Blagrave, K., Bouffard, D., et al. (2022). Long-term ice phenology records spanning up to 578 years for 78 lakes around the Northern Hemisphere. *Scientific Data*, *9*(1), 318. https://doi.org/10.1038/s41597-022-01391-6

Skamarock, W. C., & Coauthors. (2008). A description of the Advanced Research WRF version 3. *NCAR Tech. Note NCAR/TN-475+STR*, 113.

Smagorinsky, J. (1963). General circulation experiments with the primitive equations: I. The basic experiment. *Monthly Weather Review*, *91*(3), 99–164. https://doi.org/10.1175/1520-0493(1963)091<0099:gcewtp>2.3.co;2

U.S. National Ice Center. Naval ice center. Retrieved from www.natice.noaa.gov/products/great_lakes.html (accessed on 11 Nov 2023).

Wake, A., & Rumer, R. R. (1979). Effect of surface meltwater accumulation on the dissipation of lake ice. *Water Resources Research*, *15*(2), 430–434. https://doi.org/10.1029/wr015i002p00430

Wang, J., Hu, H., Schwab, D., Leshkevich, G., Beletsky, D., Hawley, N., & Clites, A. (2010). Development of the great lakes ice-circulation model (GLIM): Application to Lake Erie in 2003–2004. *Journal of Great Lakes Research*, *36*(3), 425–436. https://doi.org/10.1016/j.jglr.2010.04.002

Wang, J., Kessler, J., Bai, X., Clites, A., Lofgren, B., Assuncao, A., et al. (2018). Decadal variability of Great Lakes ice cover in response to AMO and PDO, 1963–2017. *Journal of Climate*, *31*(18), 7249–7268. https://doi.org/10.1175/jcli-d-17-0283.1

Yao, T., Tang, C. L., & Peterson, I. K. (2000). Modeling the seasonal variation of sea ice in the Labrador Sea with a coupled multicategory ice model and the Princeton ocean model. *Journal of Geophysical Research*, *105*(C1), 1153–1165. https://doi.org/10.1029/1999jc900264